

## A Density Functional Theory Study of Additives in Electrolytes of a Dye Sensitized Solar Cell

Maeng-Eun Lee,<sup>†</sup> Moon-Sung Kang,<sup>‡</sup> and Kwang-Hwi Cho<sup>§,\*</sup>

<sup>†</sup>R&D Center, Samsung SDI Co., LTD, Yongin, Gyeonggi-do 446-577, Korea

<sup>‡</sup>Department of Environmental Engineering, Sangmyung University, Cheonan 330-720, Korea

<sup>§</sup>Department of Bioinformatics and Life Science, Soongsil University, Seoul 156-743, Korea. \*E-mail: chokh@ssu.ac.kr

Received May 25, 2013, Accepted May 31, 2013

The effect of additives in an electrolyte solution on the conversion efficiency of a dye sensitized solar cell was investigated. A density functional theory (DFT) method was used to examine the physical and chemical properties of nitrogen-containing additives adsorbed on a TiO<sub>2</sub> surface. Our results show that additives which cause lower partial charges, higher Fermi level shifts, and greater adsorption energies tend to improve the performance of DSSCs. Steric effects that prevent energy losses due to electron recombination were also found to have a positive effect on the conversion efficiency. In this work, 3-amino-5-methylthio-1*H*-1,2,4-triazole (AMT) has been suggested as a better additive than the most popular additive, TBP, and verified with experiments.

**Key Words** : Dye-sensitized solar cells (DSSCs), Additive, Electrolyte, DFT, Atomistic simulation

### Introduction

Dye-sensitized solar cells (DSSCs) have been widely studied due to their potential as environment-friendly products, their simple assembly technology, and low cost.<sup>1,2</sup> Because of their various colors, transparency, wide range of operation temperatures and wide angle of incident light, DSSCs have been attracting much attention for various applications.<sup>3-6</sup> However, in spite of the many advantages of DSSCs, the energy conversion efficiency has been lower than that of Si-based solar cells. The photo-to-current conversion efficiency of DSSCs was approximately 11% under AM 1.5 (100 mW/cm<sup>2</sup>) irradiation.<sup>7-9</sup> However, using graphitic thin films embedded with highly dispersed titanium dioxide (TiO<sub>2</sub>) nanoparticles improves cell efficiency in some limited conditions.<sup>10</sup> In DSSCs, electrolytes play an important role in determining the cell performances. In general, a higher conversion efficiency of DSSC was obtained when an electrolyte was used together with proper additives. Additives such as nitrogen-containing compounds, *e.g.* 4-*tert*-butylpyridine (TBP), are added to the electrolytes to enhance the open-circuit photovoltage ( $V_{oc}$ ) and thus the conversion efficiency ( $\eta$ ) of DSSCs.<sup>11-14</sup>

Recently, much research into improving the conversion efficiency of DSSCs has been attempted by incorporating additives in the electrolyte solution.<sup>15-19</sup> However, most additives have been selected based on trial and error experiments. We have applied a computational method to find efficient additives for the electrolyte solution. The effect of additives on the TiO<sub>2</sub> surface were investigated with Density Functional Theory (DFT). Then, the results are compared with experimental data to examine the correlation between the effect of additives and DSSC cell performance. Computational characteristic features of additives which affect

the efficiency of DSSCs have been identified in order to find better additives. With the findings, a new nitrogen-containing additive has also been suggested and verified with experiments.

The efficiency of DSSCs could be affected by the complicated interaction of TiO<sub>2</sub>, dyes, electrolytes and additives. However, in order to see the effect of additives, our research has been focused on the physical properties of additives and the interaction with TiO<sub>2</sub>, which the additives bind to.

### Experimental

**Computer Simulation.** Our simulation systems were designed by adsorbing an additive molecule on the TiO<sub>2</sub> surface to understand how this adsorbed additive affects the TiO<sub>2</sub> surface. Nitrogen-containing additives such as pyridine, 4-*tert*-butyl pyridine (TBP), 1,2,4-triazole, imidazole, guanidine, 3-amino-1*H*-1,2,4-triazole (3ATz) and 3-amino-5-methylthio-1*H*-1,2,4-triazole (AMT) are considered and shown in Figure 1.

The geometries of all additives shown in Figure 1 were optimized using Gaussian 03 at the DFT/6-31G\* level.<sup>20</sup> Atomic charges were calculated using the Natural Population Analysis (NPA) method.<sup>21-23</sup> The TiO<sub>2</sub> lattice is constructed by a periodic box with  $a = 10.8 \text{ \AA}$ ,  $b = 7.5 \text{ \AA}$ ,  $c = 9.3 \text{ \AA}$  and  $\alpha = 90^\circ$ ,  $\beta = 90^\circ$ ,  $\gamma = 90^\circ$ . Periodic surface slabs with a 15  $\text{\AA}$  vacuum region were also used for the TiO<sub>2</sub> anatase (1 0 1) surface<sup>24,25</sup> and additives are added in the vacuum region to represent complex systems of additives and TiO<sub>2</sub>. In order to obtain the Fermi level energies and adsorption energies, the density functional theory (DFT) calculation was performed using CASTEP<sup>26-28</sup> in Materials Studio 4.4 from Accelrys Inc. The generalized gradient corrected (GGA) function by Perdew, Barke, and Ernzerhof (PBE)<sup>29</sup> was employed in the DFT calculation.

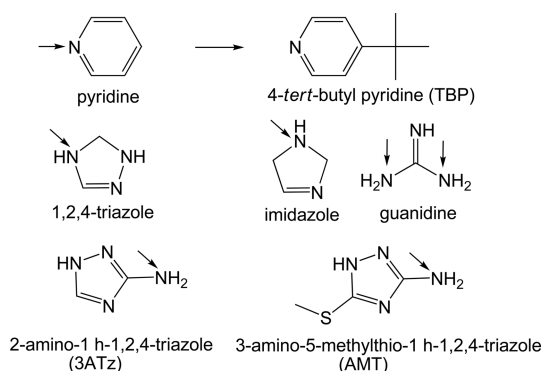


**Figure 1.** The structures of the nitrogen containing additives considered. The arrows indicate the atom with the lowest partial charge.

**Electrolyte Preparation.** The liquid electrolytes were prepared by dissolving 0.62 M 1-butyl-3-methylimidazolium iodide (BMImI), 0.05 M  $I_2$ , and 0.1 M LiI in acetonitrile (ACN). We have tested 7 additives in total, *i.e.* pyridine, 4-*tert*-butylpyridine (TBP), 1,2,4-triazole, imidazole, guanidine, 3-amino-1*H*-1,2,4-triazole (3ATz), 3-amino-5-methylthio-1*H*-1,2,4-triazole (AMT), for enhancement of the photovoltaic properties of DSSC. They were added into the electrolytes with a concentration of 0.5 M for evaluation. All chemicals except BMImI (CTRI, Korea) were purchased from Aldrich and utilized without further purification.

**DSSC Preparation.** DSSCs were fabricated according to the following procedure: Transparent conductive oxide glass (TCO, sheet resistance =  $7 \Omega/\square$ ) was employed to prepare both the photoanode and counter electrodes. For the photoanode preparation, commercial  $TiO_2$  paste (E&B Korea) was cast onto the TCO substrate using a doctor-blade technique and successively sintered at 500 °C for 30 min. A Platinum layered counter electrode was prepared by a conventional sputtering method. The photoelectrodes were sensitized with  $Ru(dcbpy)_2(NCS)_2$  dye (here, dcbpy = 2,2'-bipyridyl-4,4'-dicarboxylato) solution (5,3,5-bis TBA, Solaronix, dissolved in ethanol) overnight.

**Characterization of Photovoltaic Performances of DSSCs.** The photovoltaic characteristics of the prepared DSSCs (short-circuit current ( $J_{sc}$ ), open-circuit voltage ( $V_{oc}$ ), fill factor ( $ff$ ) and overall energy conversion efficiency ( $\eta$ )) were evaluated under 1 sun light intensity ( $100 \text{ mW cm}^{-2}$ , AM1.5G), checked with an NREL-calibrated Si-solar cell (PV Measurements Inc.).

## Results and Discussion

Table 1 represents the performance of a dye-sensitized solar cell measured by experiment. The conversion efficiency ( $\eta$ ),  $V_{oc}$  and  $J_{sc}$  of different additives are compared (including no-additives) in an electrolyte solution. As seen in Table 1, when an additive is added into the electrolyte solution, the conversion efficiency is relatively increased.

Table 2 shows the physical and chemical properties calculated from our computer experiments. The lowest partial

**Table 1.** The conversion efficiency ( $\eta$ ), open-circuit photovoltage ( $V_{oc}$ ) and short-circuit current ( $J_{sc}$ ) measured experimentally

Additives	$\eta$ (%)	$V_{oc}$ (V)	$J_{sc}$ (mA/cm <sup>2</sup> )
No additive	5.42	0.65	12.33
Pyridine	5.92	0.65	12.70
TBP	8.58	0.71	15.79
1,2,4-Triazole	6.11	0.64	15.81
Imidazole	6.53	0.79	11.76
Guanidine	7.46	0.68	15.88
3ATz	8.49	0.73	17.15
AMT	9.05	0.70	18.29

**Table 2.** The lowest partial charges, binding energies, Fermi energies which are obtained by simulations

Additives	Charge <sup>a</sup>	$E_{ad}$ <sup>b</sup>	$E_F$ <sup>c</sup>
No additive	0	0	-1.9
Pyridine	-0.43	-2.38	-1.18
TBP	-0.44	-3.64	0.77
1,2,4-Triazole	-0.49	-1.64	-1.31
Imidazole	-0.56	-2.03	-0.85
Guanidine	-0.81	-3.32	1.3
3ATz	-0.85	-1.84	-0.03
AMT	-0.85	-2.08	0.51

<sup>a</sup>The lowest partial charge. <sup>b</sup>adsorption energy in eV. <sup>c</sup>Fermi energy in eV.

atomic charge of each additive molecule, the adsorption energy between an additive and a  $TiO_2$  surface, and the  $TiO_2$  Fermi energy are obtained with a DFT calculation. These simulated properties are compared with experimental data to find dominant factors that are correlated with the DSSCs cell performance.

Figure 2 represents the correlation between the lowest partial charge and Fermi energy. As the lowest partial charge of additives is increased, a  $TiO_2$  Fermi level energy is also increased. When an additive was adsorbed on a  $TiO_2$  surface,

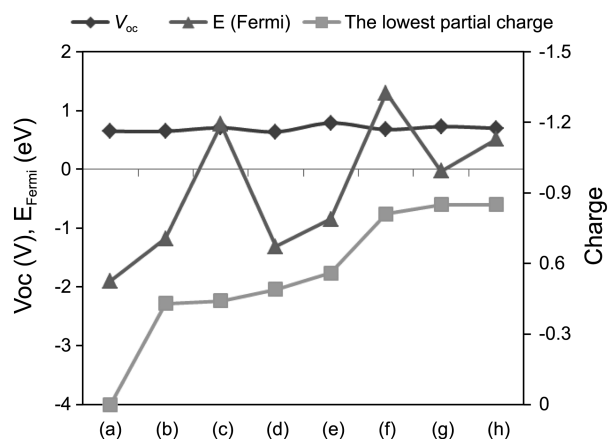


**Figure 2.** Correlation of  $V_{oc}$  (diamond), the Fermi energy (triangle) and lowest partial charge (square) with the additive species. (a) No additive, (b) Pyridine, (c) TBP, (d) 1,2,4-Triazole, (e) Imidazole, (f) Guanidine, (g) 3ATz, and (h) AMT.

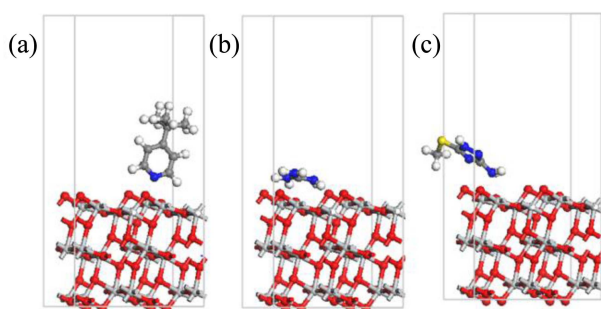


**Figure 3.** The optimized geometries of additives adsorbed on a  $\text{TiO}_2$  surface: (a) TBP, (b) Guanidine, (c) AMT.

the  $\text{TiO}_2$  Fermi energy was negatively shifted. (We follow the experimenters' convention in calling the upward shift in the Fermi energy a 'negative shift'.) In particular, the Fermi energies of the TBP, guanidine and AMT are dramatically increased with an increase of the lowest partial charges.

Additives such as TBP, guanidine and AMT have specific features in their molecular structure that maximize the spatial covering area, so that it prevents the energy loss from  $\text{TiO}_2$  to electrolytes. This may explain why they induce such a large shift in the  $\text{TiO}_2$  Fermi energies.

As seen in Figure 3, when the geometries of guanidine and AMT adsorption on a  $\text{TiO}_2$  surface were optimized, their resulting adsorption orientation allowed for all of the electron-donating sites such as nitrogen to be closer to the  $\text{TiO}_2$  surface. This is in contrast to the other additives which adsorb vertically onto the  $\text{TiO}_2$  surface, as seen by the example of TBP shown in Figure 3(a). However, unlike the other additives, the *tert*-butyl functional group in TBP still allows for a large coverage of the  $\text{TiO}_2$  surface. Therefore, TBP, guanidine and AMT additives give rise to a stronger electron-donating effect on the  $\text{TiO}_2$  surface, and thus can induce a larger negative shift of Fermi energy than others.

In this work, we observed that electron donating properties such as partial charges of additives have an influence on the Fermi level energy. However, contrary to the reports in previous works,<sup>18</sup> we cannot find any correlation between  $V_{oc}$  and Fermi energy. Except for the 1,2,4-triazole additive, when an additive is added to the electrolyte solution, the  $V_{oc}$  is increased relatively compared to the  $V_{oc}$  of the electrolyte solution with no additives. And, the  $\text{TiO}_2$  Fermi energy obtained by simulation also increased. This means that an additive adsorbed on a  $\text{TiO}_2$  surface enhances the  $\text{TiO}_2$  Fermi energy and the  $V_{oc}$ .

The efficiency is remarkably enhanced when TBP, 3ATz, and AMT are added to the electrolyte solution. The AMT additive represents a higher efficiency than TBP, which is widely used. And 3ATz is also a good additive to enhance the efficiency. In spite of the highest Fermi energy shift of guanidine, its efficiency is not the highest. This result shows that factors other than the Fermi energy contribute to the conversion efficiency. Apart from this one exception, the trends in Figure 4 show a strong correlation between the Fermi energy and the conversion efficiency.

Another finding of this work is the effect of adsorption

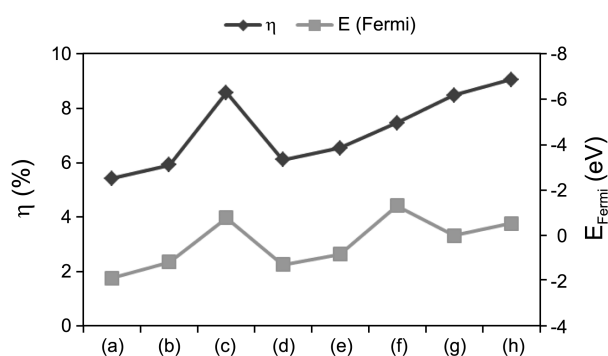


**Figure 4.** The relationship between the Fermi level (eV) obtained by simulation and the conversion efficiency (%) in an experiment. (a) No additive, (b) Pyridine, (c) TBP, (d) 1,2,4-Triazole, (e) Imidazole, (f) Guanidine, (g) 3ATz, and (h) AMT.

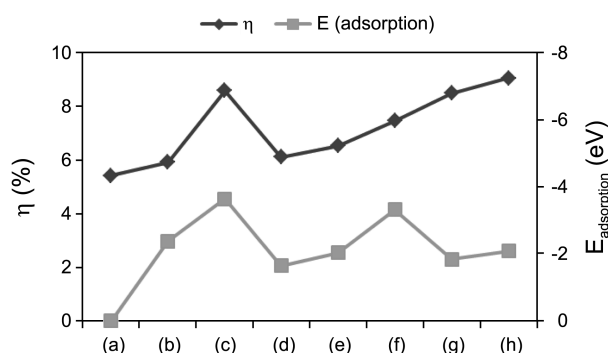


**Figure 5.** The correlation between the adsorption energy (square) obtained by simulation and the efficiency (diamond) in experiment.

energy on the conversion efficiency of DSSCs. Figure 5 represents the correlation between the adsorption energy (eV) and conversion efficiency (%). The greater the adsorption energies between an additive and the  $\text{TiO}_2$  surface, the higher the efficiencies, as shown in Figure 5. Also worth noting is the adsorption energy of guanidine, which is lower than the adsorption energy of TBP. This may explain the low conversion efficiency of guanidine in spite of its large Fermi level shift. In contrast, TBP meets all the high-efficiency conditions such as a large Fermi level shift, a strong adsorption energy and a good steric effect to prevent the energy loss. The highest conversion efficiency was achieved when using the AMT additive. Compared to TBP, its adsorption energy and Fermi level shift are slightly lower, but with a steric property that cause a better prevention of energy loss, AMT gives the highest conversion efficiency of the molecules we studied.

## Conclusion

Nitrogen-containing additives adsorbed on a  $\text{TiO}_2$  anatase (1 0 1) surface were investigated with DFT calculations. Our results were compared with experimental data on conversion efficiency ( $\eta$ ) and open circuit voltage ( $V_{oc}$ ). In this work, chemical and physical properties such as partial atomic charges, Fermi energy, adsorption energy and steric effect

are found to have correlations with conversion efficiency. In particular, AMT can be used as a better additive than the most popular additive, TBP. In addition to that, contrary to previous reports,<sup>18</sup> we found that there is no correlation between  $V_{oc}$  and Fermi energy.

**Acknowledgments.** This work was supported by the National Research Foundation of Korea, funded by the Ministry of Education, Science, and Technology (NRF-2012M3A9D1054705).

### References

1. O'Regan, B.; Grätzel, M. *Nature* **1991**, 353, 737.
2. Sayama, K.; Hara, K.; Mori, N.; Satsuki, M.; Suga, S.; Tsukagoshi, S.; Abe, Y.; Sugihara, H.; Arakawa, H. *Chem. Commun.* **2000**, 13, 1173.
3. Higuchi, K.; Kato, N. *R&D Review of Toyota CRDL*; Toyota, Japan, **2006**, 41(1), 51.
4. Toyoda, T.; Sano, T.; Nakajima, J.; Doi, S.; Fukumoto, S.; Ito, A.; Tohyama, T.; Yoshida, M.; Kanagawa, T.; Motohiro, T.; Shiga, T.; Higuchi, K.; Tanaka, K.; Takeda, Y.; Fukano, T.; Katoh, N.; Takeichi, A.; Takechi, K.; Hiozawa, M. *J. Photochem. Photobiol. A: Chemistry* **2004**, 164(1-3), 203.
5. Motohiro, T. *Nippon Kagakkai Koen Yokoshu* **2005**, 85(1), 614.
6. Takeda, Y.; Kato, N.; Higuchi, K.; Takeichi, A.; Motohiro, T.; Fukumoto, S.; Sano, T.; Toyoda, T. *Solar Energy Materials and Solar Cells* **2009**, 93(6-7), 808.
7. Nazeeruddin, M. K.; De Angelis, F.; Fantacci, S.; Selloni, A.; Viscardi, G.; Liska, P.; Ito, S.; Bessho, T.; Grätzel, M. *J. Am. Chem. Soc.* **2005**, 127, 16835.
8. Grätzel, M. *J. Photochem. Photobiol.* **2003**, C 4, 145.
9. Grätzel, M. *Prog. Photovolt.: Res. Appl.* **2006**, 14, 429.
10. Jang, Y. H.; Xin, Z.; Byun, M.; Jang, Y. J.; Lin, Z.; Kim, D. H. *Nano Letters* **2011**, 12, 479.
11. Greijer, H.; Lindgren, J.; Hagfeldt, A. *J. Phys. Chem. B* **2001**, 105, 6314.
12. Nazeeruddin, M. K.; Kay, A.; Rodicio, I.; Humphry-Baker, R.; Muller, E.; Liska, P.; Vlachopoulos, N.; Grätzel, M. *J. Am. Chem. Soc.* **1993**, 115, 6382.
13. Huang, S. Y.; Schlichthörl, G.; Nozik, A. J.; Grätzel, M.; Frank, A. *J. Phys. Chem. B* **1997**, 101, 2576.
14. Schlichthörl, G.; Huang, S. Y.; Spargue, J.; Frank, A. *J. Phys. Chem. B* **1997**, 101, 8141.
15. Asaduzzaman, A. M.; Schreckenbach, G. *Phys. Chem. Chem. Phys.* **2010**, 12, 14609.
16. Kay, A.; Grätzel, M. *J. Phys. Chem.* **1993**, 97, 6272.
17. Lee, K. M.; Suryanarayanan, V.; Ho, K. C.; Thomas, K. R. J.; Lin, J. T. *Solar Energy Materials & Solar Cells* **2007**, 91, 1426.
18. Kusama, H.; Kurahisge, M.; Arakawa, H. *J. Photochem. Photobiol.* **2005**, 169, 169.
19. Kusama, H.; Orita, H.; Sugihara, H. *Langmuir* **2008**, 24, 4411.
20. Frisch, M. J. et al. *Gaussian03*, 2004, Gaussian, Inc.
21. Carpenter, J. E.; Weinhold, F. *J. Mol. Struct. (Theochem)* **1998**, 169, 41-62.
22. Foster, J. P.; Weinhold, F. *J. Am. Chem. Soc.* **1980**, 102, 7211.
23. Reed, A. E.; Weinhold, F. *J. Chem. Phys.* **1983**, 78, 4066.
24. Barbe, C. J.; Arendse, F.; Comte, P.; Jirousek, M.; Lenzenmann, F.; Shklover, V.; Grätzel, M. *J. Am. Ceram. Soc.* **1997**, 80, 3157.
25. Park, N. G.; van de Lagemaat, J.; Frank, A. *J. Phys. Chem. B* **2000**, 104, 8989.
26. White, J. A.; Bird, D. M. *Phys. Rev. B* **1994**, 50, 4954.
27. Hohenberg, P.; Kohn, W. *Phys. Rev. B* **1964**, 136, 864.
28. Levy, M. *Proc. Natl. Acad. Sci. U. S. A.* **1979**, 76, 6062.
29. Perdew, J. P.; Burke, K.; Ernzerhof, M. *Phys. Rev. Lett.* **1996**, 77, 3865.